Linear Exchange Model for the Description of Mass Transfer Limited Bioavailability at the Pore Scale

FALK HESSE,*,† HAUKE HARMS,‡ SABINE ATTINGER,†,§ AND MARTIN THULLNER‡,||

Department of Computational Hydrosystems, UFZ-Helmholtz Centre for Environmental Research, Leipzig, Germany, Department of Environmental Microbiology, UFZ-Helmholtz Centre for Environmental Research, Leipzig, Germany, Institute of Geoscience, University of Jena, Jena, Germany, and Department of Earth Sciences−Geochemistry, Utrecht University, Utrecht, The Netherlands

Received August 18, 2009. Revised manuscript received January 26, 2010. Accepted January 28, 2010.

Reactive transport simulations are a common approach for the quantitative assessment of contaminant biodegradation in the subsurface. To use knowledge on microbial kinetics for the simulation of in situ biodegradation, the mass transfer processes controlling the bioavailability of the contaminants need to be described appropriately. A common approach to account for this problem is using a linear exchange model controlling the link between bulk and bioavailable concentration. Assuming that the subsequent degradation is controlled by the bioavailable concentration, only, these two steps can be combined to an analytical expression for the overall reaction rate know as the Best-Equation. In our work, we evaluate this approach for its ability to describe biodegradation kinetics limited by pore-scale mass transfer. Results from explicit numerical and analytical simulations of mass transport and reactive consumption at the pore scale are used to test the accuracy of results obtained using the Best-Equation. Our analysis shows that strictly spoken the Best-Equation is not valid. However, a good approximation can be achieved with errors of less than 6% in cases of moderate bioavailability and much lower errors in cases of either low or high bioavailability. These results support the description of mass transfer processes used in many reactive transport models. Furthermore, we present a method to obtain an accurate estimate of the unknown rate parameter controlling the diffusive mass transfer processes at the pore scale.

Introduction

In the last years, in situ bioremediation has become a common remediation strategy for sites contaminated by organic carbon species (*1*). It is obvious that the effectiveness of such an approach is mainly dependent on the ability of groundwater microorganisms to metabolize the respective contaminant. Measured degradation rates in the field, however, have been shown to be often much lower than those under idealized laboratory conditions (*2, 3*). This observed discrepancy has led to the concept of bioavailability, i.e. the contaminant may not be fully available to be degraded by the microorganisms. No single definition of bioavailability exists (*4, 5*). Due to the complex structure of the subsurface and the variety of processes controlling the fate of reactive species, factors influencing the bioavailability range from the physical and chemical state of the species to mass transfer limitations taking place at different scales or across the cell membrane (*6*−*9*).

In this study, we focus on pore-scale mass fluxes. The relevance of these processes for biodegradation is still under discussion, while some have argued in favor (*10*−*12*), and some against it (*13*). Nonetheless, different concepts have been proposed to account for these pore-scale mass fluxes. Many of these studies assume that macroscopic degradation kinetics follow the same type of rate law as at the pore scale. Commonly these models use a first-order reaction rate (*14*−*16*), but recently more advanced studies with Monod respectively Michaelis−Menten kinetics have been presented (*12, 17, 18*). However, these models showed problems, when trying to give a rigorous mathematical justification for the effective parameters. As an alternative, approaches relying on a two-step scheme for the pore-scale mass transfer have been shown to describe bioavailability at the pore scale with good accuracy (*19, 20*). In these models, a distinct separation between the macroscopically measured or bulk concentration and the microscopically bioavailable concentration is assumed. Since only the latter is subject to biodegradation, the microbial degradation activity is linked to the bioavailable concentration by Monod respectively Michaelis−Menten kinetics. The mass flux between these two concentrations is described by a linear exchange term. Under steady state conditions, it can be combined with the reaction kinetics into a single analytical expression for the macroscopic reactive flux. This expression is known as the Best-Equation (*21*). An intrinsic problem when using a linear exchange term is the assumption of the mass exchange taking place between two distinct compartments or reservoirs of the subsurface (e.g., pore water with bulk concentration and a biophase with bioavailable concentration). A clear separation of both however, is not possible for porous media with laminar flow fields.

In this work, we use a simple representation of a single pore to simulate transport and biodegradation of a chemical species at the pore scale. The degradation reaction at the surface of the pore is assumed to follow Michaelis−Menten kinetics. A subsequent averaging over the pore will yield an effective description of the degradation process. These averaged results will serve as references for descriptions of the macroscopic degradation rate using the Best-Equation. With this approach we aim to verify (i) whether the effective reaction kinetics can be described by the Best-Equation and thus whether the linear exchange model provides an adequate description of pore-scale mass transfer processes, (ii) how the mass transfer coefficient to be used in the linear exchange model can be estimated for a given scenario, (iii) how the accuracy and applicability of this method is compared to macroscopic Michaelis−Menten kinetics, and (iv) under which circumstances pore-scale mass fluxes must be considered. The results from this study will therefore assess the applicability of the linear exchange model for the quantitative

* Corresponding author e-mail: falk.hesse@ufz.de.
† Department of Computational Hydrosystems, UFZ-Helmholtz Centre for Environmental Research.
‡ Department of Environmental Microbiology, UFZ-Helmholtz Centre for Environmental Research.
§ University of Jena.
|| Utrecht University.

10.1021/es902489q

Published on Web 02/22/2010

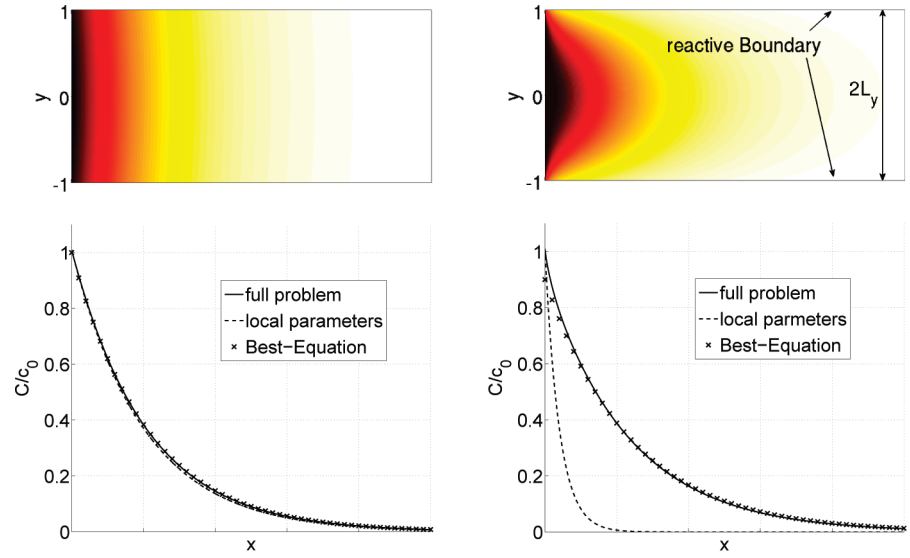

(a) Reaction-limited regime ($\Phi^2 \ll 1$) (b) Diffusion-limited regime ($\Phi^2 \gg 1$)

FIGURE 1. (top) Selected examples showing simulated concentration distributions for the full problem for two different scenarios. (bottom) Comparison of averaged numerical simulations (—) of the full problem to solutions of eq 16 using the Best-Equation with a fitted j_{tr} (×) and using Michaelis−Menten kinetics with local reaction rate parameters (- - -).

description of pore-scale mass transfer limitations on bioavailability.

Theory

Biodegradation at the Pore Scale. In this study, it is assumed that in porous media microorganisms are bound to the surface of the solid matrix and thus biodegradation of dissolved chemical species can only take place at the interface between the fluid phase carrying the dissolved species and the solid matrix phase of the medium. In contrast to the continuum approach used to describe processes at the macroscale, pore-scale descriptions allow for a clear separation between the fluid and the solid phase. Assuming that microorganisms are homogeneously covering the fluid−solid interface at no growth conditions, the fate of biodegradable species is given by the pore-scale solution of the advection−diffusion−reaction equation:

$$\frac{\partial c}{\partial t} = -\nabla\cdot(\mathbf{v}c) + D\Delta c + R \tag{1}$$

Here, $\mathbf{v}$ describes the water flow velocity and c the species concentration, both subject to pore-scale variations. D is the molecular diffusion coefficient. The reaction rate R describes the biodegradation taking place at the fluid−solid interface, only:

$$R = \begin{cases} 0 & \text{in the fluid phase} \\ -a_v q_{max}\dfrac{c}{K_m + c} & \text{at the fluid−solid interface} \end{cases} \tag{2}$$

Here, q_{max} is the maximum surface reaction capacity (given in mass per surface area and time, determined by the density and degradation capability of the microorganisms covering the surface), a_v is the specific reactive surface, and K_m is the Michaelis constant. This allows us to express the maximum reaction rate as

$$k_{max} = a_v q_{max} \tag{3}$$

Note that under the constraint of a homogeneous steady-state biomass coverage of the surface, the Michaelis−Menten kinetics given by eq 2 is structurally identical to the Monod expression.

Pore-scale Geometry. The domain used for the calculations is a semi-infinite two-dimensional channel with diameter $2L_y$ and the fluid−solid interface presented by the (reactive) wall of the channel (see Figure 1 top and the Supporting Information for more details). For a realistic porous medium, this domain could be applied in a network model consisting of capillary tubes (*22, 23*). Although the features of interest for this study are comprised in the used domain, effects like tortuosity, pore connectivity, and a modulated pore diameter are not considered here. However, simplified pore geometries like the one used herein have been shown to yield insight into the dependency of geometry, transport, and reaction in general (*24*) as well as reactive transport at the pore scale (*16, 25, 26*).

Mass Transfer Described by a Linear Exchange Term. As an alternative to calculating biodegradation rates by solving eqs 1 and 2 explicitly at the pore-scale, introducing a linear exchange term allows for a simplification of the problem. The general concept is to distinguish between two individual concentrations (representing two individual reservoirs): (i) the bulk concentration C (interpreted as the weighted average of the concentration along the width of the pore) which is affected by transport and (ii) the bioavailable concentration c_{bio} (interpreted as the concentration at the pore wall) which determines the rate of biodegradation. Both concentrations are coupled using a linear exchange term R_{tr} to describe the mass exchange rate

$$R_{tr} = a_v j_{tr}(C - c_{bio}) \tag{4}$$

Here, j_{tr} is the mass flux coefficient allowing to define the mass transfer rate coefficient k_{tr} as

$$k_{tr} = a_v j_{tr} \tag{5}$$

This approach is also known as the linear driving force model first proposed by Glueckauf and Coates (*27*) for adsorption chromatography (*28*), which has been used from then on in the field of reactive transport, too (*29, 30*). Since in a channel geometry this mass exchange takes place in a direction transversal to the water flow and is driven by diffusion, one might anticipate that

$$k_{tr} \propto \frac{D}{L_y} \tag{6}$$

Despite its simplicity, the predictive capacity of the approach given by eq 4 is limited due to the difficulties when trying to establish a connection between k_{tr} and real physical features of the porous medium (see e.g. the work of Dykaar and Kitanidis (*15*) for a detailed discussion). Therefore, we cannot infer further properties of this parameter at this point of the study.

Using eq 4, eqs 1 and 2 can be rewritten as

$$\frac{\partial C}{\partial t} = -V_{eff}\nabla C + D_{eff}\Delta C - R_{tr} \tag{7}$$

and

$$\frac{\partial c_{bio}}{\partial t} = R_{tr} - k_{max}\frac{c_{bio}}{K_m + c_{bio}} \tag{8}$$

with D_{eff} as effective diffusion coefficient and V_{eff} as the effective transport velocity along the length of the pore channel. For the calculation of these quantities, we refer to the work of Balakotaiah and Chang (*14*) and Heβe et al. (*18*). Note that V_{eff} is equal to the average pore velocity V for high bioavailability and increases by a maximum factor of approximately 1.4 for very low bioavailability (*18*). Relaxation times at the pore scale can be considered short compared to macro-scale fluctuations of flow velocities and species concentrations, which justifies the assumption of steady state conditions. Using this assumption, eqs 7 and 8 can be further simplified to a single equation describing the change of the bulk concentration along the pore channel:

$$\frac{\partial C}{\partial t} = -V_{eff}\nabla C + D_{eff}\Delta C - R_{Best} = 0 \tag{9}$$

with

$$R_{Best} = \frac{K_m k_{tr}}{2}\left(1 + \frac{C}{K_m} + \frac{k_{max}}{K_m k_{tr}}\right) \times \left(1 - \sqrt{1 - \frac{4\frac{C}{K_m}\frac{k_{max}}{K_m k_{tr}}}{\left(1 + \frac{C}{K_m} + \frac{k_{max}}{K_m k_{tr}}\right)^2}}\right) \tag{10}$$

The latter is the so-called Best-Equation Best (*21*) derived by inserting eq 4 into eq 8 and rearraging under steady state conditions (i.e., $R_{tr} = R_{Best}$, $\partial c/\partial t = 0$; see, e.g., the works of Simoni et al. (*2*) or Bosma et al. (*19*) for a more detailed discussion). Note that in eqs 8 and 10, k_{max} and k_{tr} are given by eqs 3 and 5, respectively. The Best-Equation provides a closed expression for the biodegradation rate with respect to the macroscopic or bulk concentration C. This macroscopic reaction rate is the result of two consecutive microscopic processes: the diffusive mass transfer and a local reactive consumption (the consumption at the microscopic location of the microorganisms, i.e. the solid water interface). Depending on the prevalence of these processes, the macroscopic rate will be either diffusion- or reaction-limited, or a combination of both.

Dimensionless Description. In order to obtain generalizable results and to make use of mathematical concepts derived previously by Heβe et al. (*18*), the above variables and equations are transferred into dimensionless descriptions. For this purpose, reference lengths, $L_{x,ref}$ and $L_{y,ref}$, as well as a reference concentration c_{ref} are used. For $L_{y,ref}$, we choose half the width of the pore (see the schematic in the Supporting Information), and $L_{x,ref}$ is a characteristic length scale of the contaminant along flow paths, which is certainly much longer than $L_{y,ref}$. As c_{ref}, the concentration at the pore inlet is chosen. Using these references, allows for the definitions of the Péclet number, and the Thiele modulus, as dimensionless numbers or scaling units. The Péclet number

$$Pe = \frac{V{L_{y,ref}}^2}{D L_{x,ref}} \tag{11}$$

is a measure for the relevance of advective versus diffusive mass fluxes. The Thiele modulus (*31*) is defined as

$$\Phi^2 = \frac{k_{max} L_{y,ref}}{a_v D K_m} \tag{12}$$

and is a measure to assess whether the macroscopic reaction rate is controlled by the local reaction rate or by diffusive fluxes.

Applying these above reference values allows to transfer all system variables into a dimensionless form

$$\hat{c}, \hat{K}_m = \frac{c, K_m}{c_{ref}}, \quad \hat{q}_{max} = q_{max}\frac{L_{y,ref}}{D c_{ref}}, \quad \hat{j}_{tr} = j_{tr}\frac{L_{y,ref}}{D}, \quad \hat{x} = \frac{x}{L_{x,ref}}, \text{ and } \quad \hat{y} = \frac{y}{L_{y,ref}} \tag{13}$$

Description of the Full Problem. By assuming the constraint ${L_{y,ref}}^2 \ll {L_{x,ref}}^2$, justified above, we can neglect the longitudinal diffusion (*18, 25, 26*). Furthermore, we can state that the velocity field has only a component in the direction of the flow path (see the figure in the Supporting Information). Using this assumption and the definitions above, eqs 1 and 2 can be converted into the following dimensionless steady-state expressions for the investigated pore channel:

$$Pe\left(1 - \frac{y^2}{L_y}\right)\frac{\partial}{\partial \hat{x}}\hat{c} = \frac{\partial^2}{\partial \hat{y}^2}\hat{c} \tag{14}$$

in the fluid phase, and

$$\nabla \hat{c} \cdot \mathbf{n} = -\Phi^2 \frac{\hat{c}}{1 + \hat{c}/\hat{K}_m} \tag{15}$$

at the fluid−solid interface. The velocity distribution in eq 14 is defined as a parabolic function and $\mathbf{n}$ is the outer unit normal.

Note that, unless stated otherwise, we will use only dimensionless variables in the remainder of the manuscript. For the sake of simplicity, we will thus drop the circumflex accent above the symbols.

Effective Problem Description. Applying the above dimensionless variables to eqs 9 and 10 also allows expressing the effective solution for the pore-space geometry in dimensionless form:

$$\frac{V_{eff}}{V}\frac{\partial}{\partial x}C - \frac{D_{eff}}{D}\frac{\partial^2}{\partial x^2}C = a_v \frac{Q}{Pe} \tag{16}$$

with Q as the dimensionless form of the Best-Equation:

$$Q = \frac{j_{tr} K_m}{2}\left(1 + \frac{C}{K_m} + \frac{\Phi^2}{j_{tr}}\right) \times \left(1 - \sqrt{1 - \frac{4\frac{C}{K_m}\frac{\Phi^2}{j_{tr}}}{\left(1 + \frac{C}{K_m} + \frac{\Phi^2}{j_{tr}}\right)^2}}\right) \tag{17}$$

For the derivation and the calculation of the effective transport parameters in eq 16, we refer again to the work of Balakotaiah and Chang (*14*) or Heβe et al. (*18*) (valid for $Pe < 10$).

For comparison, an alternative expression was considered for Q in eq 16 using effective Michaelis−Menten kinetics in analogy to previous studies (*17, 18*) (denominated as Monod kinetics therein):

$$Q = \frac{\Phi_{\text{eff}}^2 C}{1 + C/K_{\text{m,eff}}} \tag{18}$$

with the effective reaction parameters Φ_{eff}^2 and $K_{\text{m,eff}}$ being linked to the local values for Φ^2 and K_{m} either using a single scaling parameter η_{eqv} with $\Phi_{\text{eff}}^2 = \eta_{\text{eqv}}\Phi^2$ and $K_{\text{eff}} = \eta_{\text{eqv}}K_{\text{m}}$ (*17, 18*) or using two independent scaling parameters $\eta_{1,\text{eqv}}$ and $\eta_{2,\text{eqv}}$ with $\Phi_{\text{eff}}^2 = \eta_{1,\text{eqv}}\Phi^2$ and $K_{\text{eff}} = \eta_{2,\text{eqv}}K_{\text{m}}$ (*18*).

General Approach. To evaluate the applicability of the linear exchange model, numerical solutions of the full problem description given by eqs 14 and 15 are compared to solutions of the effective problem description given by eq 16.

Numerical solutions of the full problem were obtained using a finite element solver (for further details see the work of Radu et al. (*32*)). A parabolic profile was considered as velocity distribution along the width of the pore channel, and at the inflow of the pore channel, a fixed concentration c_0 was used as a boundary condition.

The resulting two-dimensional concentration distribution is subsequently averaged over the transversal axis to obtain a one-dimensional concentration profile along the longitudinal flow path. This concentration profile was used as a reference for the results of the effective problem descriptions. Due to physically unrealistic boundary conditions at the inlet, we avoided artifacts by excluding regions close to the inlet from the fitting procedure. In order to make all following analysis compareable, we chose as criteria the point, where the cross section of the concentration distribution is well-approximated by a single cosine function (see also refs *14*, *16*, or *18* for further details). Solutions of the effective problem were obtained applying a Runge−Kutta solver. Values for the unknown mass flux coefficient j_{tr} in eq 17 and the scaling factor(s) $\eta_{*,\text{eqv}}$ in eq 18 were determined by fitting, i.e. minizing the square sum error between the analytically derived one-dimensional concentration profile (Best-Equation) and the one obtained by numerical simulation. Furthermore, values for j_{tr} were estimated analytically making use of results from Heβe et al. (*18*) (see the Supporting Information for a detailed description).

Results and Discussion

To demonstrate the general approach and to indicate the relevance of using an appropriate effective description, results are first shown for two arbitrary examples: one representing a reaction-limited regime (Figure 1a), where the macroscopic degradation rate is mainly controlled by the local reaction rate, and one representing a diffusion-limited regime (Figure 1b), where mainly transversal diffusive fluxes are controlling the macroscopic degradation rate. Numerical simulation results (steady state) of the full problem show that for the reaction-limited regime concentration gradients along the width of the pore channel are rather smooth (Figure 1a top). This results in the average bulk concentration C being representative for the concentration at the pore wall c_{bio}. As a consequence, the bulk concentration profile along the length of the pore obtained by averaging the numerical results along the width of the pore channel can be reasonably well predicted using an effective description with Michaelis−Menten kinetics and the local parameters (i.e., using eq 16 with Q as in eq 18 and $\eta_{1,\text{eqv}} = \eta_{2,\text{eqv}} = 1$) (Figure 1a bottom). In contrast, for the diffusion-limited regime, strong concentration gradients can be observed along the width of the pore, and the bulk concentration C differs from the concentration at the pore wall c_{bio} (Figure 1b top). In this case, predicting the longitudinal bulk concentration profile using Michaelis−Menten kinetics with local parameters leads to an overestimation of the macroscopic reaction rate and thus to an underestimation of the bulk concentration (Figure 1b bottom). For both regimes, using an effective description based on the linear exchange model, i.e. using the Best-Equation as the effective reaction rate Q in eq 16, allows for a very good reproduction of the longitudinal bulk concentration profile (Figure 1 bottom) indicating the general applicability of the approach.

General Behavior of the Mass Flux Coefficient j_{tr}. In order to assess the general behavior and the accuracy of the linear exchange model, the above comparison of results from numerical simulations of the full problem and from the effective solution using the Best-Equation was performed for a broad range of possible scenarios characterized by different values of the Thiele modulus Φ^2 and the ratio between the maximum concentration and the Michaelis constant c_0/K_{m}. While Φ^2 is a good inverse measure for the relative importance of reactive vs diffusive processes, the ratio c_0/K_{m} indicates if the reaction rate is (initially) following (i) an effective zeroth-order regime ($c_0/K_{\text{m}} \gg 1$), (ii) an effective first-order regime ($c_0/K_{\text{m}} \ll 1$), or (iii) a transition between both ($c_0/K_{\text{m}} \approx 1$).

Optimum fit results obtained for j_{tr} show a dependency of this parameter on the local reaction rate parameters (i.e., Φ^2 and c_0/K_{m}) (Figure 2a). With respect to Φ^2, different regimes can be identified: for low values of Φ^2, j_{tr} shows a strong dependency on c_0/K_{m} with higher values of c_0/K_{m} associated with higher values of j_{tr} resulting in a variation of j_{tr} over several orders of magnitude (Figure 2a, left part), which have been reported before by Young and Ball (*33*) for similar setups. In contrast, for sufficiently high values of Φ^2 optimum fit values approach a constant value of $j_{\text{tr}} \approx 2.4-2.5$ independent of c_0/K_{m} (Figure 2a right part). The transition between these two extremes is characterized by j_{tr} increasing with Φ^2 toward a maximum value before decreasing toward the constant value for large Φ^2. The larger c_0/K_{m}, the larger the value of Φ^2 at which maximum values of j_{tr} are reached and at which subsequently the constant value is approached.

The residual errors obtained when comparing one-dimensional concentration profiles determined by fitting j_{tr} to solutions of the full problem show that for both, very high or very low values of Φ^2, the Best-Equation provides a very good estimate of the concentration along a pore-scale flow path with negligible errors (Figure 2b). For values of $\Phi^2 \approx 10^0-10^2$, larger errors can be observed, the value of which depend on c_0/K_{m}. For high values of c_0/K_{m}, errors of up to 2.5% can be found, with decreasing maximum values with decreasing c_0/K_{m}. Also values of Φ^2 at which highest errors were found depend on c_0/K_{m} with higher c_0/K_{m} shifting the peak of the residual error toward higher values of Φ^2.

Given that a value of $c_0/K_{\text{m}} = 0.1$ represents the first-order range of Michaelis−Menten kinetics, the Best-Equation appears to be most accurate for this type of reaction regime. However, as maximum errors remain below 3% for all combinations of c_0/K_{m} and Φ^2, the Best-Equation provides a good effective description also for the zeroth-order range of Michaelis−Menten kinetics and the transition between these extremes. This indicates that in general the linear exchange model is an adequate effective description of bioavailability limited biodegradation at the pore-scale. However, for low Φ^2, values of j_{tr} obtained by fitting varied over several orders of magnitude depending on both, Φ^2 and c_0/K_{m}. This would certainly challenge the prediction of j_{tr} and the applicability of the linear exchange model for practical use.

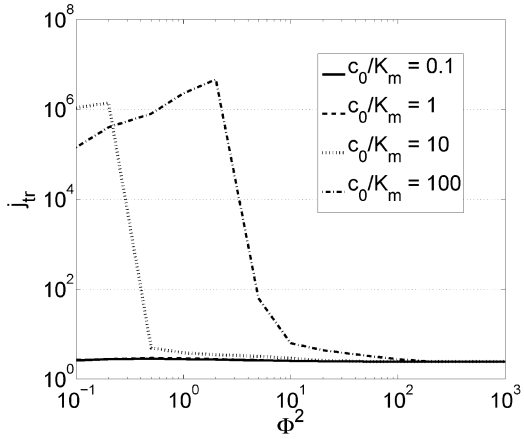

(a) Optimum fit values for j_{tr}.

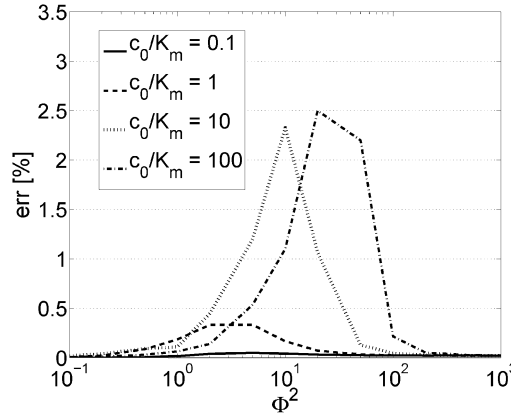

(b) Residual errors after fitting using a optimum fit for j_{tr}.

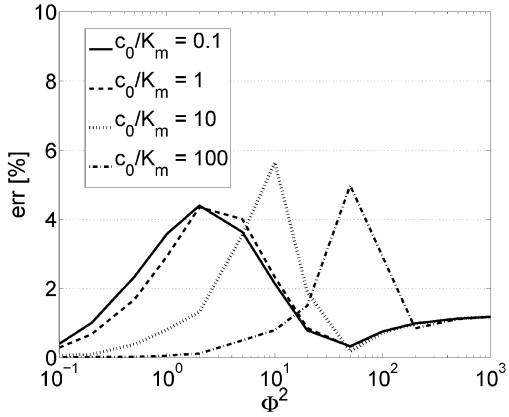

(c) Residual errors after fitting using a constant estimate for j_{tr}.

FIGURE 2. Behavior and accuracy of the mass flux coefficient j_{tr} from eq 17 with respect to Φ^2. The value of j_{tr} was determined by fitting an effective solution using eq 16 to averaged numerical solutions of the full problem for several Φ^2 and c_0/K_m (a, b).

Using a Constant Estimate for j_{tr}. As discussed in the above section, j_{tr} showed strong variations with respect to the parameters of the local reaction rate, i.e. Φ^2 and c_0/K_m (Figure 2a). For high values of Φ^2 and/or low values of c_0/K_m however, the mass flux coefficient j_{tr} appeared to be relatively constant. In addition, sensitivity analysis showed that for high c_0/K_m, results are rather insensitive even to large variations of j_{tr} (data not shown). These observations are consistent with the fact that for high c_0/K_m a zeroth-order reaction regime is prevailing with the reaction rate hardly depending on concentration. Thus, j_{tr} controlling the link between bulk and bioavailable concentration is not supposed to have a major impact on the overall reaction rate, which explains the low sensitivity. In contrast, for low c_0/K_m representing a first-order reaction regime, the concentration is considered to be a crucial factor for the overall degradation rate and consequently the sensitivity toward j_{tr} is higher. As a consequence, any value for j_{tr} which might be used to represent the entire range of Φ^2 and c_0/K_m values should be at first a good estimate for the first-order regime.

A reanalysis of the results from Heβe et al. (*18*) allows for low values of c_0/K_m to derive an analytical estimate of

$$j_{tr} = \pi^2/4 \approx 2.47 \tag{19}$$

(see the Supporting Information for a detailed derivation). This value is identical to results of Haggerty and Gorelick (*34*) reported for the case of layered diffusion, and is also nearly identical to the optimum fit values found for large Φ^2. In order to assess the applicability of this constant estimate for the entire range of Φ^2 and c_0/K_m, an error analysis was done in analogy to the above section (Figure 2b).

Results of this error analysis for a constant value of $j_{tr} = \pi^2/4$ show again a good accuracy with small errors in the cases of either low or high values of Φ^2 (Figure 2c). Higher errors are again observed in the transition regime with values showing a dependency on Φ^2 and c_0/K_m compareable to above results. The maximum of this error, however, does not exceed 6% regardless of the value of c_0/K_m, which is still in an acceptable range compared to experimental accuracies (*35*). These findings support the extrapolation of the analytically determined first-order regime value of j_{tr} to the entire range of reaction regimes. Thus, the simplicity of obtaining an estimate while keeping the estimation errors in an acceptable range suggests the analytically derived value of j_{tr} to be the more efficient approach compared to the more accurate fitting procedure.

Comparison with Macroscopic Michaelis−Menten Kinetics. To compare the accuracy of the linear exchange model with effective Michaelis−Menten kinetics suggested in the literature as effective degradation rates (*17, 18*), residual errors of these different approaches were determined assuming $c_0/K_m = 10$ as for this value large errors were found (see Figure 2b and c). Results of this comparison indicate that the highest accuracy is obtained by using effective Michaelis−Menten kinetics with two independent effective parameters (Figure 3). This observation can be attributed to the additional degree of freedom in this fitting approach compared to the

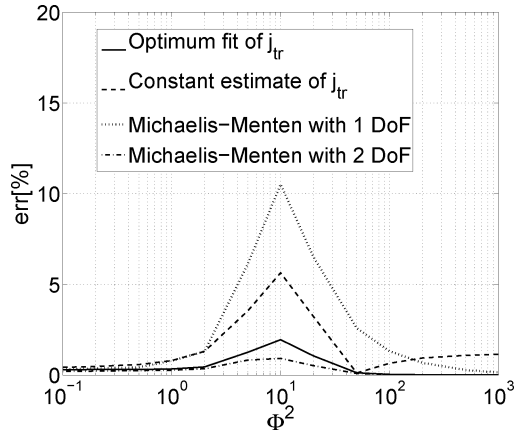

FIGURE 3. Residual errors made by using different effective rate expressions: the Best-Equation with a constant $j_{tr} = \pi^2/4$ (dashed line) and with fitted values for j_{tr} (solid line) and Michaelis−Menten kinetics with one (dotted line) and two (dashed−dotted line) degrees of freedom (DoF), i.e. independently fitted scaling parameter(s). Results were obtained assuming a value of $c_0/K_m = 10$.

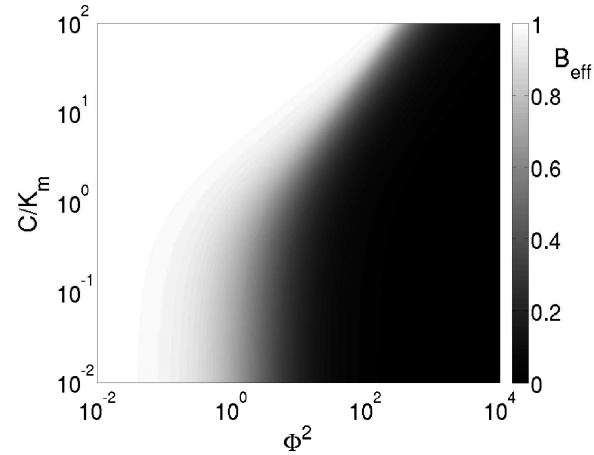

FIGURE 4. Effective bioavailability B_{eff} with respect to the local reaction rate parameters Φ^2 and C/K_m. The values were calculated as the ratio of the reactive flux given by the Best-Equation using eq 17 compared to the reactive flux given by Michaelis−Menten kinetics using eq 18 with local parameters.

expressions using a single fitting parameter. Of those approaches using one parameter only, the Best-Equation with a fitted j_{tr} is the most accurate. The analytically derived value of $j_{tr} = \pi^2/4$ leads to slightly less accurate estimates as shown above. Compared to these two estimates using the Best-Equation, effective Michaelis−Menten kinetics with only one scaling factor leads to the highest estimation errors.

Relevance of Pore-scale Bioavailability Restrictions. In order to assess the necessity of the application of an effective description for pore-scale mass fluxes, one has to evaluate the bioavailability with respect to the local reaction rate parameters Φ^2 and K_m. To quantify bioavailability Bosma et al. (*19*) introduced the bioavailability number *Bn* as the ratio between the mass transfer rate coefficient k_{tr} and the microbial specific affinity given by k_{max}/K_m. Combining this with eqs 5, 12, and 19 allows to express *Bn* as

$$Bn = \frac{k_{tr}}{k_{max}/K_m} = \frac{\pi^2}{4\Phi^2} \tag{20}$$

This relation supports the idea that the Thiele modulus can serve as a measure for species bioavailability (*36*). However, as discussed above, the relevance of such mass transfer limitations also depends on the concentration of the reactive species, an effect already reported previously (*20, 37*). For these reasons, Kampara et al. (*20*) introduced the effective bioavailability B_{eff} as the ratio between the effective degradation rate given by the Best-Equation (eq 17 using the constant estimate for j_{tr}) and the potential degradation rate in the absence of any bioavailability restrictions given by Michaelis−Menten kinetics (eq 18 using local values for Φ^2 and K_m; see the Supporting Information for more details). Expressing B_{eff} as function of Φ^2 and C/K_m (Figure 4) allows the determination of parameter combinations for which bioavailability effects need to be considered at the pore scale.

Results of this analysis show that for low concentrations ($C/K_m \leq 1$), bioavailability restrictions become relevant at values of $\Phi^2 \approx 1$ with higher Φ^2 resulting in severe bioavailability limitations of the degradation rate (Figure 4). For higher concentrations, i.e. ($C/K_m \geq 1$), values of Φ^2, for which bioavailability effects have to be expected, increase. As a result, a reduced bioavailability is confined to relatively fast reactions (high Φ^2), only. These findings are also in general agreement with the results for surface catalyzed abiotic reactions reported recently by Li et al. (*13*) who observed only negligible limitations of mineral dissolution rates at for $\Phi^2 \leq 1$ (estimate based on data given therein).

Comparison to Experimental Data. In order to illustrate the application of the concept outlined above for the interpretation of experimental data, we here use results from a column experiment on the biodegradation of 3-chlorodibenzofuran taken from the work of Harms and Zehnder (*38*) as an example. Detailed information on the setup and the experimentally determined parameters are provided in the Supporting Information, where we furthermore show how dimensionless and dimensional parameters are transferred into each other to exemplify the application of our results to real world problems.

For this experimental setup, a Thiele modulus $\Phi^2 = 1.6$ and a mass transfer rate coefficient of $k_{tr} = 0.23\ s^{-1}$ were calculated. Measured substrate concentrations decrease from 1.55 μM at the inlet to 0.37 μM at the outlet of the column which corresponds to values for C/K_m to vary between 6.7 and 1.6. Referring to the scheme given in Figure 4, this corresponds to a scenario with mildly limited bioavailability. According to Heβe et al. (*18*), these values furthermore yield an effective transport velocity $v_{eff} \approx 1.2$ larger than the average flow velocity *V*. Using the given parameter values (see the Supporting Information), the column experiment was simulated using the Biogeochemical Reaction Network Simulator (BRNS) (*39, 40*). The simulation of biodegradation of the substrate using Michaelis−Menten kinetics with the given local parameters and no correction to the flow velocity resulted in an outflow concentration of $C_{out} = 0.048\ \mu M$. This is a massive underestimation of the measured outlet concentration of $C_{out} = 0.37\ \mu M$, which indicates a limited bioavailability of the substrate in the column. When using the Best-Equation, i.e. eq 10 with the above k_{tr} and given parameter values, the simulated outlet concentration clearly increased to $C_{out} = 0.185\ \mu M$ but still underestimated the measured value. However, when deriving the hydraulic radius not from the specific surface of the glass bead packing ($r_{hyd} = 0.016$ cm; see the Supporting Information), but arbitrarily assuming it to be equal to the (upper range) of the reported glass bead size ($r_{hyd} = 0.050$ cm), the Thiele modulus increases to $\Phi^2 = 4.8$ and the mass transfer coefficient deceases to $k_{tr} = 0.073\ s^{-1}$. With these values, an outlet concentration of $c_{out} = 0.35\ \mu M$ was simulated, which is in close agreement to the measured value while the results using the local parameter Michaelis−Menten rate expression were not affected by the change of hydraulic radius. Apparently, some limitation of

bioavailability can be attributed to the diffusive mass transfer at the pore scale, but other factors (e.g., heterogeneities of the flow field, distribution of the bacteria, etc.) may have limited the bioavailability in this experiment as well.

Future research (e.g., comparing porous media packings with different bead sizes) must show if these effects can be confirmed by experimental data.

Implications for Practical Applications. The pore-scale mass transfer limitations investigated in the present study represent an intrinsic upper limit of mass transfer influenced bioavailabilty to be found in porous media. Any additional mass transfer limitation at a larger scale would lead to a reduction of the mass transfer rate coefficient. The need to consider pore-scale mass transfer limitations in practical applications is linked to the Thiele modulus Φ^2 and the ratio of C/K_m as shown above. The determination of the mass flux coefficient using a fitting routine requires however a suitable reference especially with regard to its strong dependency on the parameters of the local reaction kinetics. To avoid this limitation, a constant estimate of $j_{tr} = \pi^2/4$ can be used as an alternative with only slightly less accuracy.

Alternative approaches using Michaelis−Menten kinetics as the effective degradation rate are also challenged by the effective parameters (i) showing a distinct dependency on the local rate parameters and (ii) requiring a fitting or complex upscaling procedure for their derivation (*17, 18*). Furthermore, an improvement of the accuracy achieved by the Best-Equation can only be obtained when using two independently scaling effective parameters. Considering that an experimental determination of biodegradable organic chemicals in the environment is typically done with an error of 10% or more (*35*), the Best-Equation with a constant value of $j_{tr} = \pi^2/4$ is the most suitable compromise between providing an accurate prediction and the effort needed to determine the relevant effective parameter. Although the Best-Equation considers only one reactant, more reactive species could be modeled by means of explicit two-step schemes, i.e. an individual transport step for each species according to the linear exchange model with a subsequent combined degradation step. To predict values for the ultimately needed mass transfer rate coefficient k_{tr} from the constant mass flux coefficient j_{tr}, only knowledge of the porous matrix geometry (hydraulic radius, specific surface) and the diffusion coefficient of the degraded substrate is needed.

Acknowledgments

This study was supported by the Helmholtz Association via the program topic "CITE-Chemicals in the Environment" and grant VG-NG-338 ("GReaT MoDE").

Supporting Information Available

Analytical estimate for the mass flux coefficient j_{tr} for an effective first-order regime and additional information on the effective bioavailabilty and on the experimental setup used in this study. This material is available free of charge via the Internet at http://pubs.acs.org.

Literature Cited

(1) Alvarez, P. J.; Illman, W. A. *Bioremediation and Natural Attenuation*; Wiley & Sons: New York, 2005.
(2) Simoni, S. F.; Schäfer, A.; Harms, H.; Zehnder, A. J. Factors affecting mass transfer limited biodegradation in saturated porous media. *J. Contam. Hydrol.* **2001**, *50*, 99–120.
(3) Alexander, M. Aging, Bioavailability, and Overestimation of Risk from Environmental Pollutants. *Environ. Sci. Technol.* **2000**, *34*, 4259–4265.
(4) Ehlers, L. J.; Luthy, R. G. Contaminant Bioavailability in Soil and Sediment. *Environ. Sci. Technol.* **2003**, *37*, 295–302.
(5) Semple, K. T.; Doick, K. J.; Jones, K. C.; Burauel, P.; Craven, A.; Harms, H. Defining bioavailability and bioaccessibility of contaminated soil and sediment is complicated. *Environ. Sci. Technol.* **2004**, *38*, 228–231.
(6) Barry, D.; Prommer, H.; Miller, C.; Engesgaard, P.; Brun, A.; Zhen, C. Modelling the fate of oxidisable organic contaminants in groundwater. *Adv. Water Resour.* **2002**, *25*, 945–983.
(7) Button, D. K. Biochemical Basis for Whole-Cell Uptake Kinetics: Specific Affinity, Oligotrophic Capacity, and the Meaning of the Michaelis Constant. *Appl. Environ. Microbiol.* **1991**, *57*, 2033–2038.
(8) Johnsen, A. R.; Wick, L. Y.; Harms, H. Principles of microbial PAH-degradation in soil. *Environ. Pollut.* **2005**, *133*, 71–84.
(9) Thullner, M.; Regnier, P.; van Cappellen, P. Modeling microbially induced carbon degradation in redox stratified subsurface environments: Concepts and open questions. *Geomicrobiol. J.* **2007**, *24*, 139–155.
(10) Gramling, C. M.; Harvey, C. F.; Meigs, L. C. Reactive Transport in Porous Media: A Comparison of Model Prediction with Laboratory Visualization. *Environ. Sci. Technol.* **2002**, *36*, 2509–2514.
(11) Raje, D. S.; Kapoor, V. Experimental Study of Biomolecular Reaction Kinetics in Porous Media. *Environ. Sci. Technol.* **2000**, *34*, 1234–1239.
(12) Meile, C.; Tuncay, K. Scale dependence of reaction rates in porous media. *Adv. Water Resour.* **2006**, *29*, 62–71.
(13) Li, L.; Steefel, C. I.; Yang, L. Scale dependence of mineral dissolution rates within single pores and fractures. *Geochim. Cosmochim. Acta* **2008**, *72*, 360–377.
(14) Balakotaiah, V.; Chang, H.-C. Dispersion of Chemical Solutes in Chromatographs and Reactors. *Philos. Trans.: Phys. Sci. Eng.* **1995**, *351*, 39–75.
(15) Dykaar, B. B.; Kitanidis, P. K. Macrotransport of biologically reacting solute through porous media. *Water Resour. Res.* **1996**, *32*, 307–320.
(16) Kechagia, P.; Tsimpanogiannis, I.; Yortsos, Y.; Lichtner, P. On the upscaling of reaction-transport processes in porous media with fast or finite kinetics. *Chem. Eng. Sci.* **2002**, *57*, 2565–2577.
(17) Wood, B.; Radakovich, K.; Golfier, F. Effective reaction at a fluid-solid interface: applications to biotransformation in porous media. *Adv. Water Resour.* **2007**, *30*, 1630–1647.
(18) Heβe, F.; Thullner, M.; Radu, F. A.; Attinger, S. Upscaling of the Advection-Diffusion-Reaction Equation with Monod Reaction. *Adv. Water Resour.* **2009**, *32*, 1336–1351.
(19) Bosma, T. N. P.; Middeldorp, P. J. M.; Schraa, G.; Zehnder, A. J. B. Mass Transfer Limitation of Biotransformation: Quantifying Bioavailability. *Environ. Sci. Technol.* **1997**, *31*, 248–252.
(20) Kampara, M.; Thullner, M.; Richnow, H. H.; Harms, H.; Wick, L. Y. Impact of Bioavailability Restrictions on Microbially Induced Stable Isotope Fractionation. 2. Experimental Evidence. *Environ. Sci. Technol.* **2008**, *42*, 6552–6558.
(21) Best, J. B. The inference of intracellular enzymatic properties from kinetic data obtained on living cells: Some kinetic considerations regarding an enzyme enclosed by a diffusion barrier. *J. Cell. Comp. Physiol.* **1955**, *46*, 1–27.
(22) Kim, D.-S.; Fogler, H. S. Biomass evolution in porous media and its effects on permeability under starvation conditions. *Biotechnol. Bioeng.* **2000**, *69*, 47–56.
(23) Thullner, M.; Zeyer, J.; Kinzelbach, W. Influence of Microbial Growth on Hydraulic Properties of Pore Networks. *Transp. Porous Media* **2002**, *49*, 99–122.
(24) Kitanidis, P. K. Analysis of macrodispersion through volume-averaging: Moment equations. *Stochastic Hydrol. Hydraul.* **1992**, *6*, 5–25.
(25) Mikelic, A.; Devigne, V.; van Duijn, C. J. Rigorous upscaling of a reactive flow through a pore, under important Peclet's and Damkohler's numbers. *SIAM J. Math. Anal.* **2006**, *38*, 1262–1287.
(26) van Duijn, C. J.; Mikelic, A.; Pop, I. S.; Rosier, C. Effective dispersion equations for reactive flows with dominant Peclet and Damköhler numbers. *Adv. Chem. Eng.* **2008**, *34*, 1–45.
(27) Glueckauf, E.; Coates, J. The Influence of Incomplete Equilibrium on the Front Boundary of Chromatograms and the Effectiveness of Separation. *J. Chem. Soc.* **1947**, 1315–1321.
(28) Villermaux, J. Chemical engineering approach to dynamic modelling of linear chromatography: a flexible method for representing complex phenomena from simple concepts. *J. Chromatogr.* **1987**, *406*, 11–26.
(29) Roberts, P. V.; Goltz, M. N.; Summers, R. S.; Crittenden, J. C.; Nkedi-Kizza, P. The influence of mass transfer on solute transport in column experiments with an aggregated soil. *J. Contam. Hydrol.* **1987**, *1*, 375–393.
(30) Harvey, C. F.; Gorelick, S. M. Temporal Moment-Generating Equations: Modeling Transport and Mass Transfer in Heterogeneous Aquifers. *Water Resour. Res.* **1995**, *31*, 1895–1911.

(31) Thiele, E. W. Relation between catalytic activity and size of particle. *Ind. Eng. Chem.* **1939**, *31*, 916–920.
(32) Radu, F. A.; Bause, M.; Prechtel, A.; Attinger, S. *A mixed hybrid finite element discretization scheme for reactive transport in porous media*; Numerical Mathematics and Advanced Applications; Springer, 2008; pp 513−520.
(33) Young, D. F.; Ball, W. P. Effects of column conditions on the first-order rate modelling of nonequilibrium solute breakthrough. *Water Resour. Res.* **1995**, *31*, 2181–2192.
(34) Haggerty, R.; Gorelick, S. M. Multiple-rate mass-transfer for modelling diffusion and surface-reactions in media with pore-scale heterogeneity. *Water Resour. Res.* **1995**, *31*, 2383–2400.
(35) *Guidance document on residue analytical methods*; Technical Report, European Commission, **2000**.
(36) Chung, G.-Y.; McCoy, B. J.; Scow, K. M. Criteria to assess when biodegradation is kinetically limited by intraparticle diffusion and sorption. *Biotechnol. Bioeng.* **1993**, *41*, 625–632.
(37) Thullner, M.; Kampara, M.; Richnow, H. H.; Harms, H.; Wick, L. Y. Impact of Bioavailability Restrictions on Microbially Induced Stable Isotope Fractionation. 1. Theoretical Calculation. *Environ. Sci. Technol.* **2008**, *42*, 6544–6551.
(38) Harms, H.; Zehnder, A. J. B. Influence of substrate diffusion on degradation of dibenzofuran and 3-chlorodibenzofuran by attached and suspended bacteria. *Appl. Environ. Microbiol.* **1994**, *60*, 2736–2745.
(39) Regnier, P.; O'Kane, J. P.; Steefel, C. I.; V., J. P. Modeling complex multi-component reactive-transport systems: Towards a simulation environment based on the concept of a Knowledge Base. *Appl. Math. Modell.* **2002**, *26*, 913–927.
(40) Thullner, M.; van Cappellen, P.; Regnier, P. Modeling the impact of microbial activity on redox dynamics in porous media. *Geochim. Cosmochim. Acta* **2005**, *69*, 5005–5019.

ES902489Q